Nano Biomed Eng
2020, 12(3): 253-261. doi: 10.5101/nbe.v12i3.p253-261.

Research Article

Synthesis, Characterization, Spectroscopic and Biological Studies of Zn(II), Mn(II) and Fe(II) Theophylline Complexes in Nanoscale

Ahmad Hussein Ismail[1], Hassanain Kamil Al-Bairmani[1], Zainab Sabri Abbas[1], Ahmed Mahdi Rheima[2]

[1]Mustansiriyah University, College of Science, Department of Chemistry, Iraq.
[2]Department of Chemistry, College of Science, Wasit University, Kut, Iraq.

Corresponding authors. E-mail: ah2042013@uomustansiriyah.edu.iq; arahema@uowasit.edu.iq

Received: Feb. 5, 2020; **Accepted:** Jul. 3, 2020; **Published:** Sep. 18, 2020

Citation: Ahmad Hussein Ismail, Hassanain Kamil Al-Bairmani, Zainab Sabri Abbas, and Ahmed Mahdi Rheima, Synthesis, Characterization, Spectroscopic and Biological Studies of Zn(II), Mn(II) and Fe(II) Theophylline Complexes in Nanoscale. *Nano Biomed. Eng.*, 2020, 12(3): 253-261.
DOI: 10.5101/nbe.v12i3.p253-261.

Abstract

Three nanocomplexes of Zn(II), Mn(II), Fe(II) with theophylline were synthesized by ultrasonic sonication method. Melting point, molar conductivity, solubility, flame atomic absorption, Fourier-transform infrared spectroscopy (FTIR), ultraviolet-visible (UV-vis) spectroscopy and C/H/N elemental analyses were used to investigate and suggest the structure of the nanocomplexes. Size and morphology of the nanocomplexes were measurement by transmission electron microscopy (TEM), ranging from 6-22 nm. Efficacy of the nanocomplexes synthesized was examined against four types of bacterial strains: Staphylococcus aureus, Bacillus subtilis (Gram-positive bacteria), Klebsiella pneumonia and Escherichia coli (Gram-negative bacteria). The results showed that all nanocomplexes had very high susceptibility to inhibit bacterial growth, as indicated by their inhibition zones between 98% and 100%.

Keywords: Nanoscale complexes; Theophylline; Ultrasonic method; bacterial strains; TEM

Introduction

Transition metal complexes (TMCs) are an interesting group for compounds that can be used in almost every division branch of chemistry and technology [1-3]. These can be tailored to a specific function through necessary adjustments of either the core metal atom or the ligand sphere. Such complexes can be integrated and used in a variety of environments in chemical or biological matrices [4]. TMCs are an essential component of the human body's structural and functional elements and play a vital role in many physiological or pathological procedures [5]. Transition metal complexes drug (TMCD) have become increasingly important in inorganic and medicinal chemistry and have attracted a great deal of attention over the past decade in drug development strategies [6]. Nanotechnology plays an important role in inorganic chemistry through the formation of nano complexes and nano oxides, which are included in many biological and industrial applications [7-18]. Theophylline (Scheme 1) transition metal complexes can be used to analyze the relationship as template compounds between metal ions and nucleic acid oxo purine bases [19]. Theophylline functions as a monodentate ligand in a neutral or fundamental

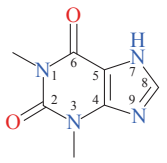

Scheme 1 Theophylline structure.

environment and coordinates metal ions through N_7 atoms [19-21]. In some instances, it functions as a bidentate N(7)/O(6) chelating ligand or as a bridging ligand with N(7)/O(6) chelation and N(9) coordination simultaneously [22]. The aim of this study was to report the synthesis and characterization of Zn(II), Mn(II) and Fe(II) nanocomplexes with theophylline as a ligand for antibacterial applications.

Experimental

Materials and methods

All chemicals and solvents used were obtained from Sigma-Aldrich. During the experimental steps, deionized water was used.

Synthesis of nanoscales complexes

Three nanoscale medical complexes were prepared following the procedure as shown in Scheme 2. The sodium salt of the medical ligand was prepared by using theophylline (0.004 mole) dissolution in 30 mL fresh NaOH (0.004 mol) solution. The obtained solution was heated up to 70 °C, and then metals (II) chloride (0.002 mol in 30 mL) were added to aqueous solution. The reaction mixture was kept under ultrasonic sonication for 3 h at 70 °C. Suitable crystals of good quality appeared at room temperature incubation after night. Filtration was used to isolate all novel complexes, washed with hot water and dried on air [19].

Characterization

Three nanoscale complexes were characterized by some devices in this study. Fourier-transform infrared spectroscopy (FTIR), flame atomic absorption and C/H/N elemental analyses, molar conductivity, solubility, and melting point were used to investigate and suggest the structure of nano complexes. The size and morphology of nano complexes were measurement by transmission electron microscopy (TEM).

Antibacterial test

Three medical nanoscales complexes of theophylline were screened for antibacterial activities by the agar diffusion method. Three samples of this complexes were dissolved in solvent dimethyl sulfoxide (DMSO) to have a solution at a concentration of 10^{-3} M for each one of these complexes and the same concentration of pure theophylline. Four types of bacterial strains, *Staphylococcus aureus, Bacillus subtilis* (Gram-positive bacteria), *Klebsiella pneumonia and Escherichia coli* (Gram-negative bacteria) were selected for this study. The approximate number of bacteria cells in agar dish was found to be 1.5×10^8 colony-forming units per milliliter by comparing it with the McFarland Standard. A cavity was made in each dish at a diameter of 5 mm to fill with the solution of medical nanoscale complexes. The dishes were incubated for a day at 37 °C. Then the inhibition zone was measured and classify.

Results and Discussion

FTIR spectra

The FTIR spectrum of theophylline in Fig. 1 shows absorption band at 3120 cm^{-1} referring to ν(NH) which disappeared in FTIR spectra of all nano complexes (Figs. 2-4), indicating that the group theophylline

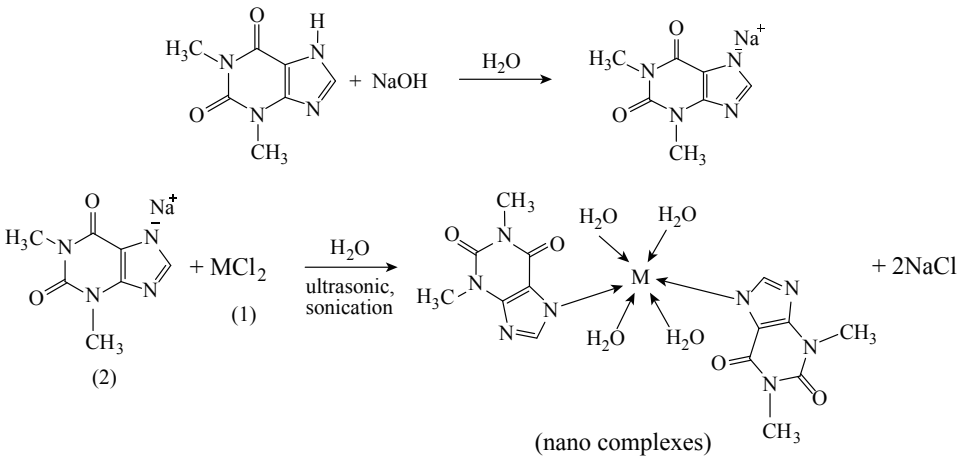

Scheme 2 Nanoscale complexes synthesized (M = Zn(II), Mn(II) and Fe(II)).

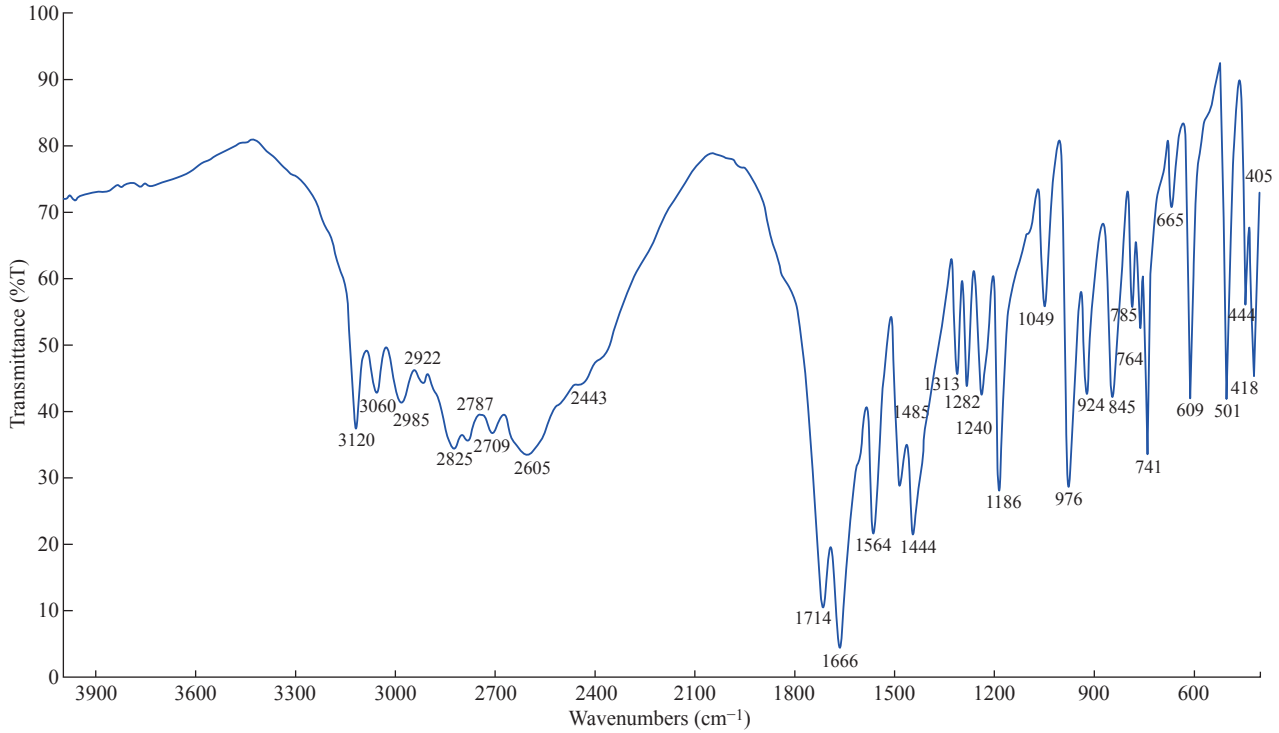

Fig. 1 FTIR spectrum of theophylline (THP).

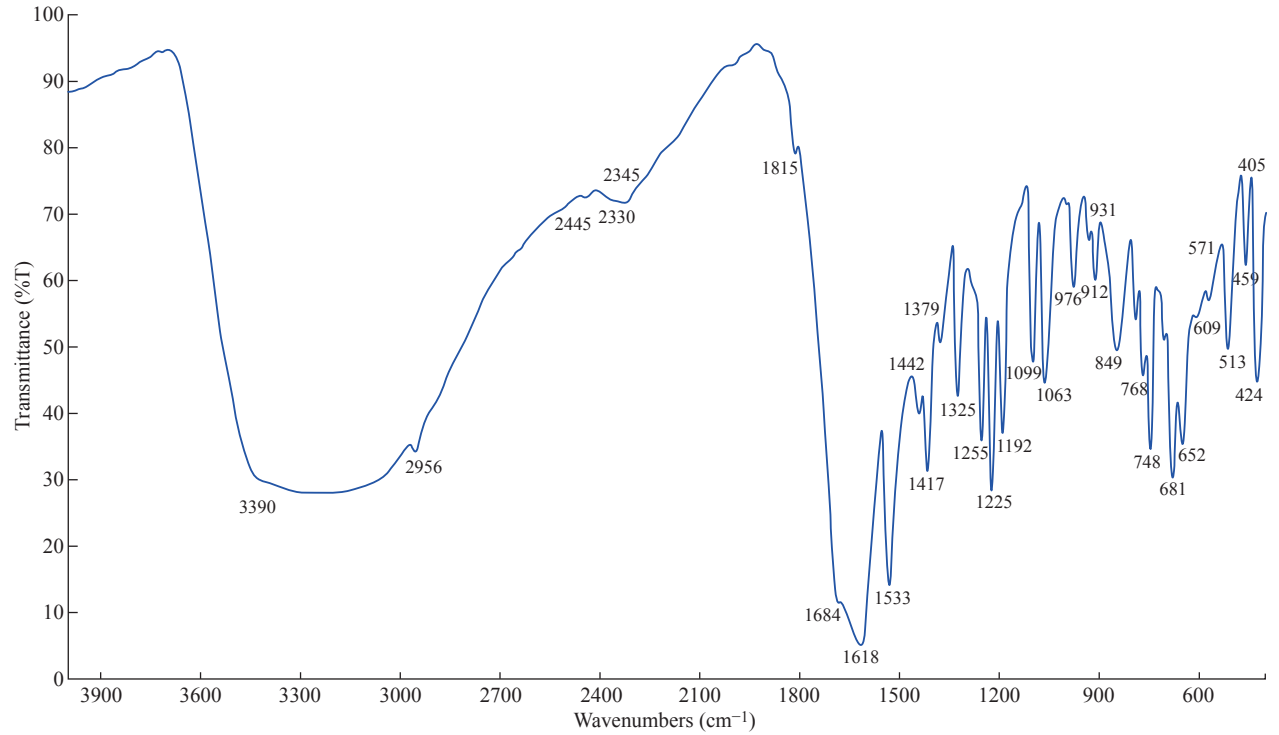

Fig. 2 FTIR spectrum of the [Zn $(THP)_2(H_2O)_4$] nano complex.

coordinated with metal ions by NH. In addition, in the region of 3390-3437 cm^{-1}, the absorption bands of all prepared complexes representing the water stretching vibration were displayed abroad, which indicated the involvement of water molecules in coordination. A new band emerged in all complexes at 569-571 cm^{-1} that referred to metal N-M coordination, with the interaction between them by coordination bond. All vibrations bands in the nano complexes were shifted to lower frequency as compared with a free theophylline due to hydrogen bonds of water molecules with the carbonyl and amine groups [23].

UV-visible spectra of the metal nano complexes

The electronic spectra for complexes were recorded in DMSO solution at room temperature with

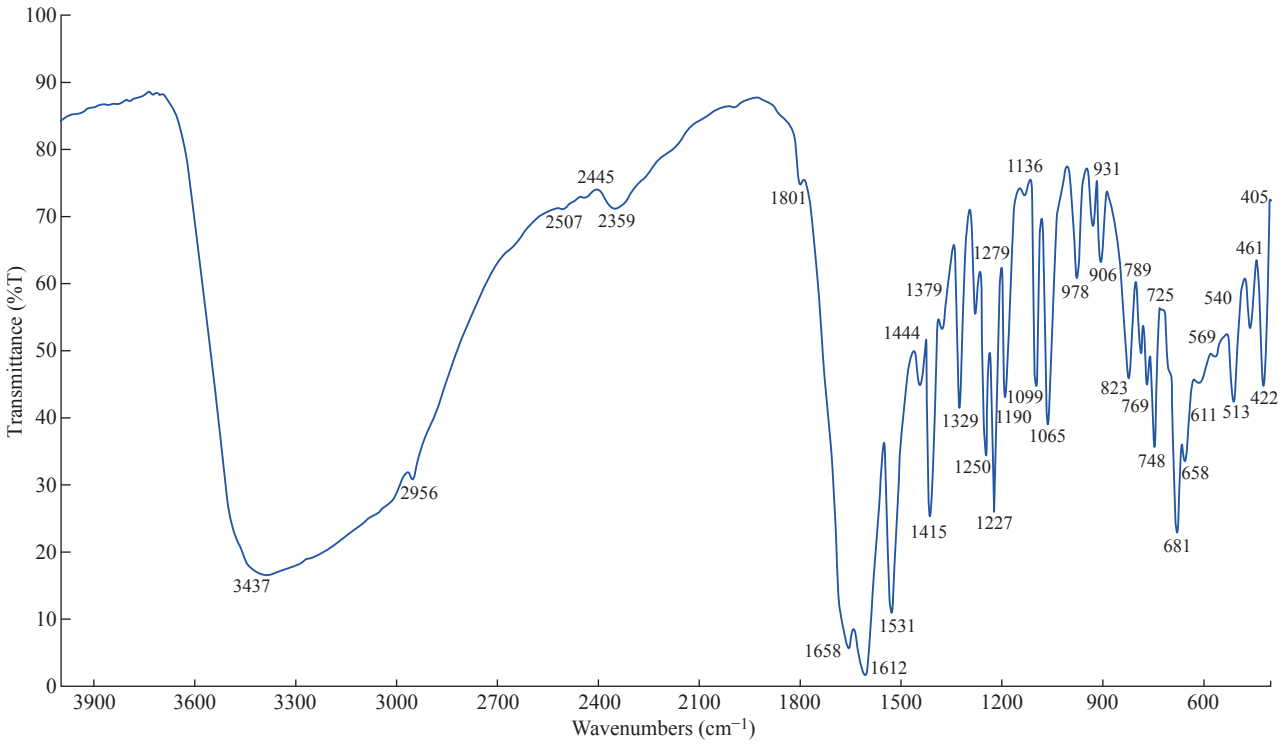

Fig. 3 FTIR spectrum of the [Mn $(THP)_2(H_2O)_4$] nano complex.

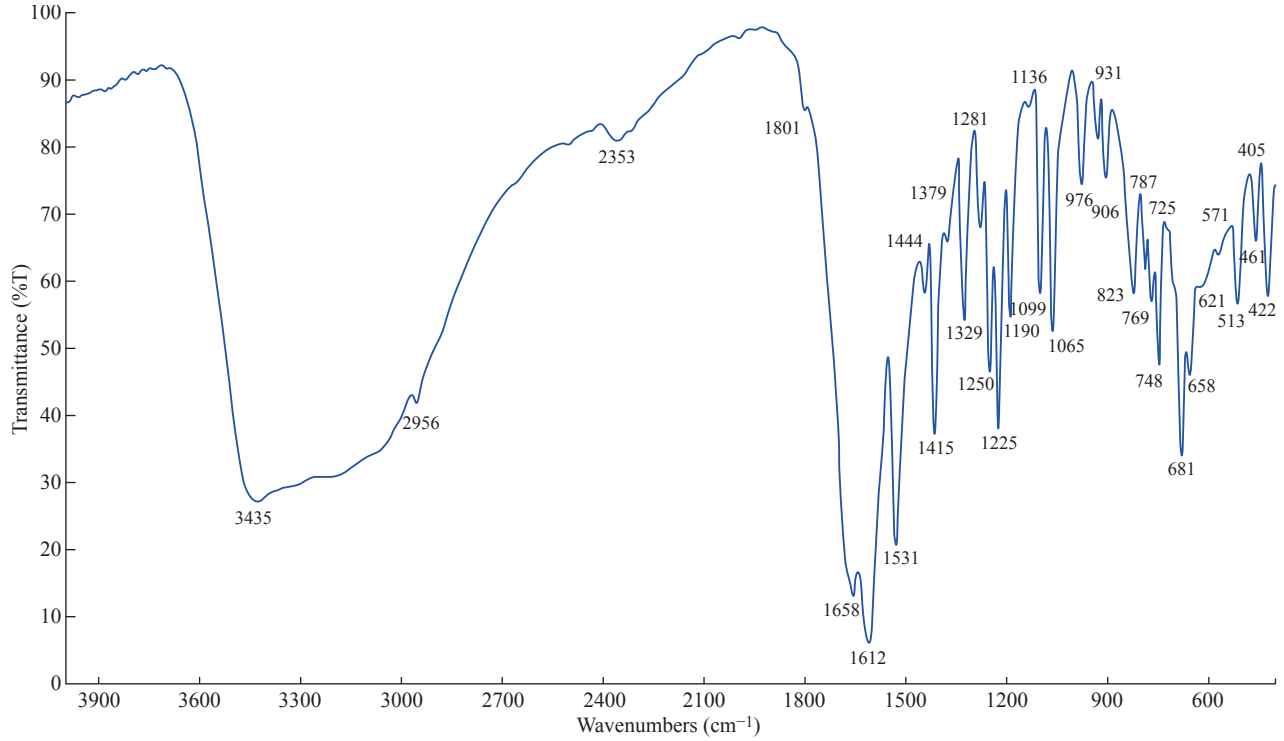

Fig. 4 FTIR spectrum of the [Fe $(THP)_2(H_2O)_4$] nano complex.

Table 1 Elemental analysis and atomic absorption spectroscopy for nano complexes

Prepared nano complexes	Molecular formula	M.wt $g \cdot mol^{-1}$	Metal analyses (%) Found (calc.)			
			C	H	N	M
[Zn $(THP)_2(H_2O)_4$]	$C_{14}H_{22}N_8O_8Zn$	495.611	33.92(32.87)	4.44(4.32)	22.61(21.94)	13.19(13.11)
[Fe $(THP)_2(H_2O)_4$]	$C_{14}H_{22}N_8O_8Fe$	486.047	34.60(34.23)	4.53(4.17)	23.05(23.1)	11.49(11.71)
[Mn $(THP)_2(H_2O)_4$]	$C_{14}H_{22}N_8O_8Mn$	485.140	34.66(33.41)	4.53(4.32)	23.1(23.13)	11.32(12.04)

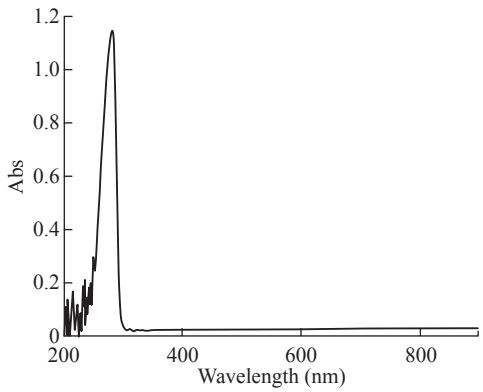

Fig. 5 The UV-Vis spectra of theophylline.

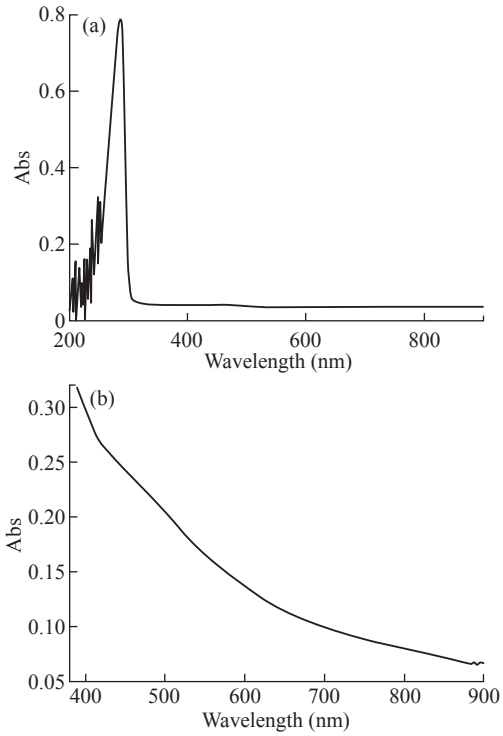

Fig. 6 (a) The UV-Vis spectra of [Mn $(THP)_2(H_2O)_4$] complex at low concentration; **(b)** visible spectra at high concentration.

wavelength ranging from 200-800 nm are shown in Figs. 5-8.

The UV-Vis spectrum of theophylline showed an absorption band at 272 nm (36764 cm^{-1}) in DMSO solvent, due to the intraligand n → π* and π→ π* transitions.

The [Mn $(THP)_2(H_2O)_4$] and [Zn $(THP)_2(H_2O)_4$] complexes did not exhibit any d-d bands in the visible region as expected for half- and fully-filled electronic configuration of the metal complexes. Depending on all previously mentioned results in addition to the results of C/H/N elemental analysis, flam atomic absorption and FTIR spectrum, we could suggest a octahedral

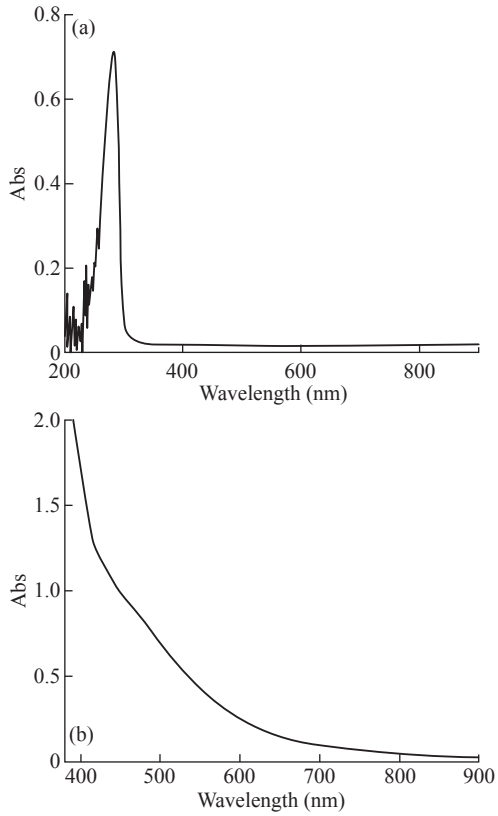

Fig. 7 (a) The UV-Vis spectra of [Zn $(THP)_2(H_2O)_4$] complex at low concentration; **(b)** visible spectra at high concentration.

geometry around the Zn(II) and Mn(II) ions.

The UV-Vis spectrum of [$Fe(THP)_2(H_2O)_4$] complex exhibited two weak absorption bands at 410 nm (24390 cm^{-1}) and 685 nm (14598 cm^{-1}) which were assigned to $^5T_2g \rightarrow {}^5Eg$ transition and charge transfer respectively. So from the data above and those obtained from FTIR spectra, C/H/N elemental analysis and flame atomic absorption, we could suggest an octahedral geometry around the Fe(II) ion [24].

Physical properties and elemental analysis of the synthesized metal nano complexes

The elemental analysis and physical properties as well as metal content of complexes are characterized in Table 1-3. The C/H/N elemental analysis was conducted to all prepared nano complexes to determine the structural molecular formula of the prepared nano

Table 2 Molar conductance and melting point of prepared nano complexes

Nano complexes	Color	M.P (°C)	Molar cond. ($S \cdot cm^2 \cdot mol^{-1}$)
[Zn $(THP)_2(H_2O)_4$]	White	297-295	15.8
[Fe $(THP)_2(H_2O)_4$]	Brown	288-286	6.3
[Mn $(THP)_2(H_2O)_4$]	Light brown	287-285	13.6

Table 3 The solubility of theophylline and nano complexes

Nano complex	DMSO	Cold water	Hot water (above 40 °C)	Acetone	EtOH	$CHCl_3$	MeOH
$[Zn (THP)_2(H_2O)_2(Cl)_2]$	++	_	+	_	+	+	+
$[Fe (THP)_2(H_2O)_2(Cl)_2]$	++	_	+	_	+	_	+
$[Mn (THP)_2(H_2O)_2(Cl)_2]$	++	_	_	_	+	_	+
Theophylline	++	_	++	_	++	+	++

Note: ++ High solubility; + Partial solubility; - Insoluble.

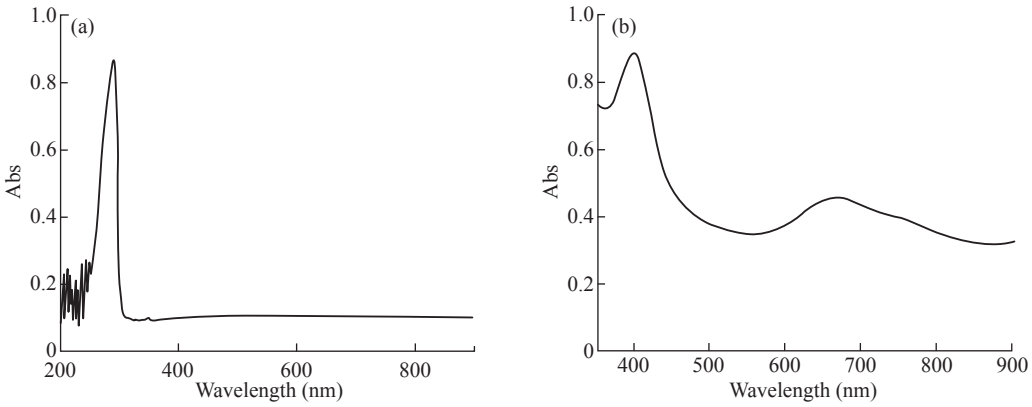

Fig. 8 (a) The UV-Vis spectra of $[Fe (THP)_2(H_2O)_4]$ complex at low concentration; **(b)** visible spectra at high concentration.

complexes through concourse of theoretical values with the practical values. The atomic absorption methods helped us in determining the metal ion percentage of the complexes. Most of these results were in good agreement with the theoretical values. The proportion of metal to ligand (2:1) octahedral structure.

Additionally, the molar conductance values of ligand and their complexes were measured in DMSO as a solvent at concentration of 10^{-3} M, where the results showed the small values of molar conductivity as of 15.8-6.3 $S.cm^2.mol^{-1}$ due to the conversion of chlorine ion into sodium chloride salt. Melting point of the ligand and their nano complexes were also measured and are shown in Table 2.

Many of solvents were used to test the solubility of nano complexes and theophylline at room temperature and as shown in Table 3.

TEM measurement

Figs. 9-11 show the transmission electron microscopy (TEM) results of all the synthesized nano complexes, which provided a clear photo with a different approximation scale. All the prepared samples

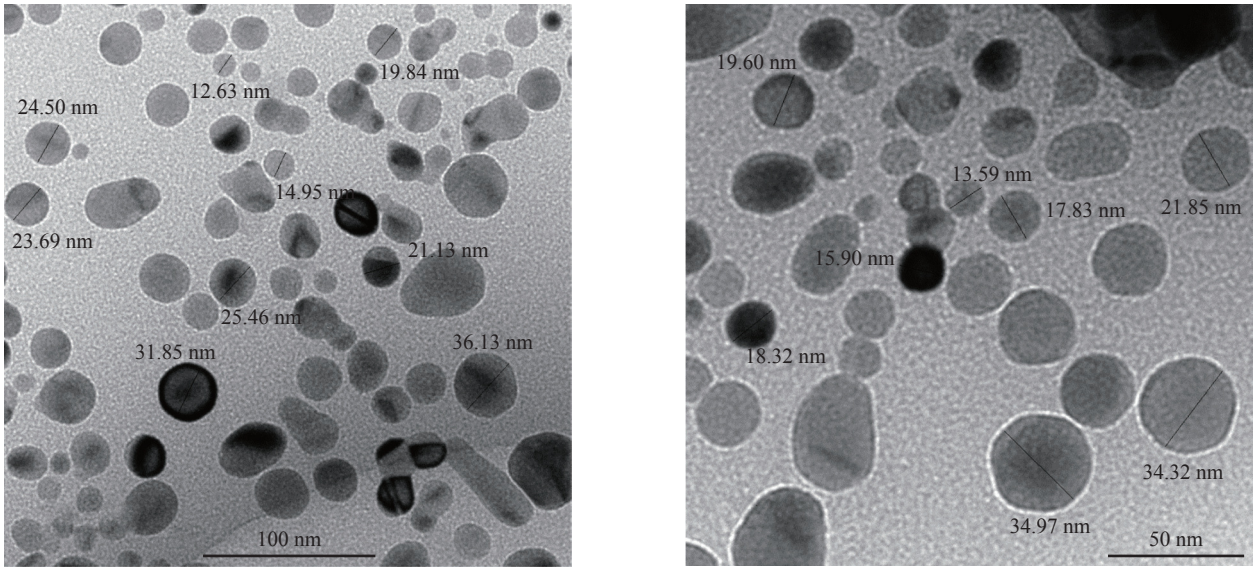

Fig. 9 TEM of $[Zn (THP)_2(H_2O)_4]$ nano complex.

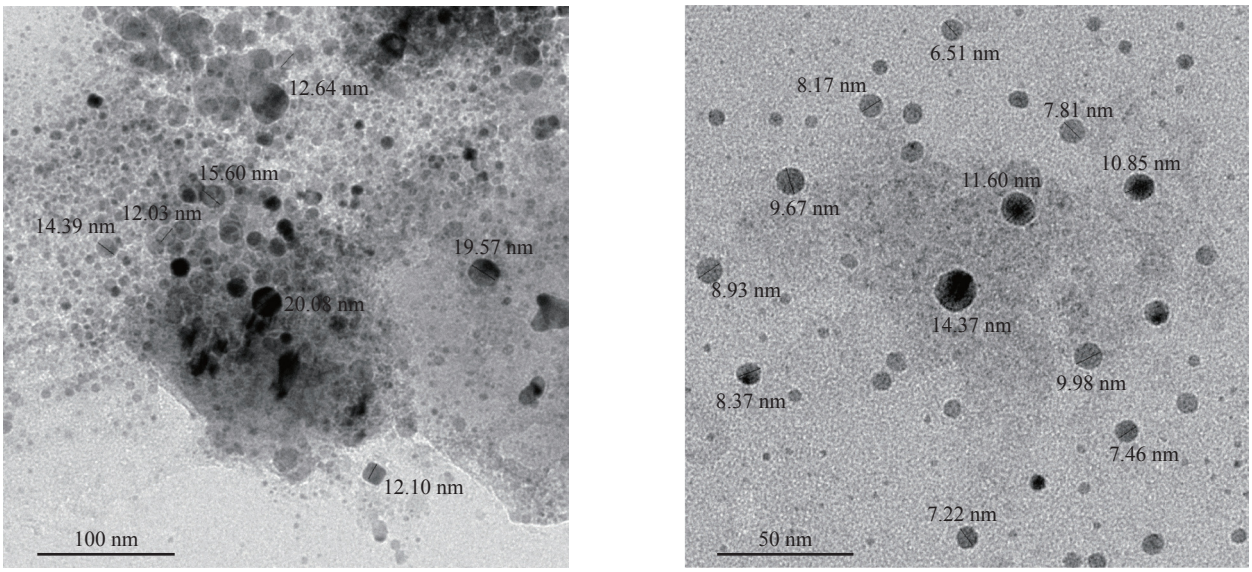

Fig. 10 TEM of [Mn $(THP)_2(H_2O)_4$] nano complex.

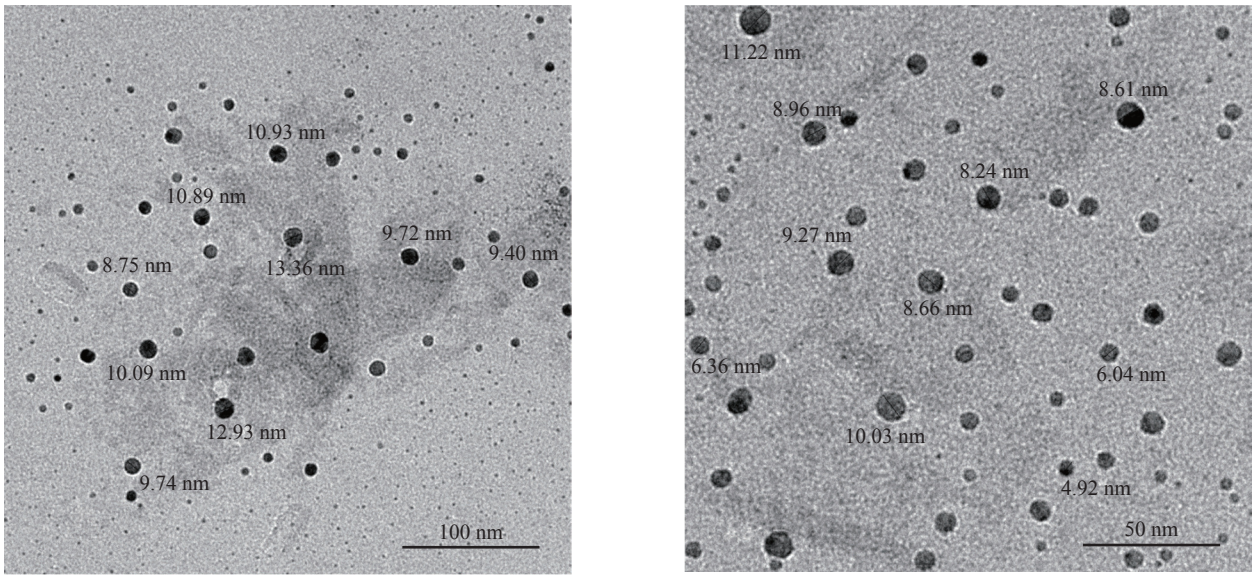

Fig. 11 TEM of [Fe $(THP)_2(H_2O)_4$] nano complex.

were free from any aggregation; all the dimensions of the synthesized complexes were within the nanoscale (less than 100 nm), indicating that the nano types were particles and zero dimensions. From the statistics, the average size was determined randomly and is shown in Table 4.

Table 4 Average size nano complexes investigated by TEM

Complex formula (nanoscale)	Average particle size (nm)
[Zn $(THP)_2(H_2O)_4$]	22
[Mn $(THP)_2(H_2O)_4$]	12
[Fe $(THP)_2(H_2O)_4$]	9

Evaluation of antibacterial activity

In the present study, the effect of nano complexes were tested against four different types of bacterial strain; *Staphylococcus aureus, Bacillus subtilis* (Gram-positive bacteria), and *Klebsiella pneumoniae, Escherichia coli* (Gram-negative bacteria). The obtained results indicated that these nano complexes exhibited excellent antibacterial activity as shown in Fig. 12. The nano complexes were able to inhibit the growth of bacteria by inhibition zone of 98-100%, as shown in Table 5. This inhibition was considered unique through killing the bacterial cell and inhibiting its growth as a result of the dispersal of the external electrical potential of its membrane, due to the high activity and high ability of the nano complexes to kill bacteria.

The zone of inhibition of the nanocomplexes at the concentration of 10^{-3} M for all tested bacteria was significant ($p < 0.01$).

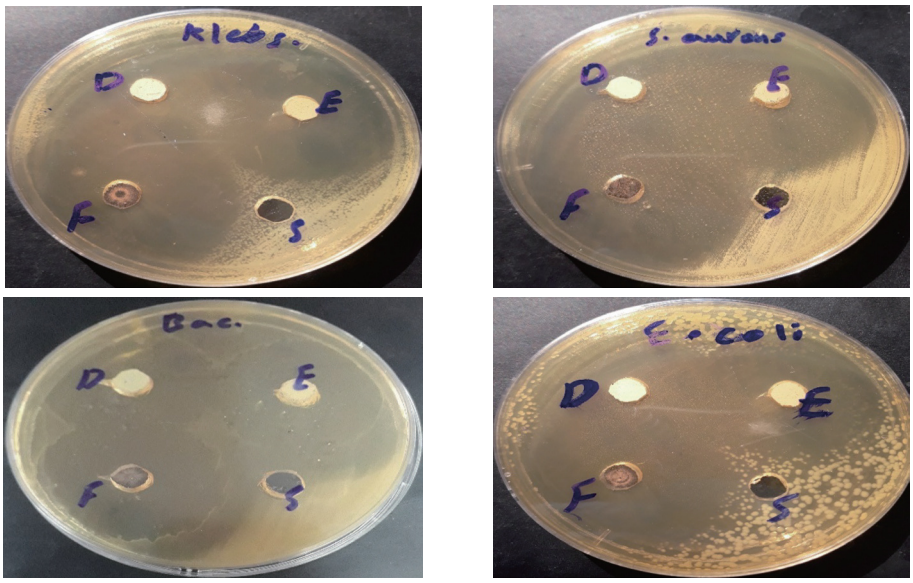

Fig. 12 The activity of nanocomplexes against four types of bacteria.

Table 5 The effect of nano complexes represented by inhibition zone (mm) against different bacterial species

Complexes formula (nanoscale)	*Staphylococcus aureus*	*Escherichia coli*	*Bacillus subtilis*	*Klebsiella pneumoniae*
$[Zn(THP)_2(H_2O)_4]$ (D)	Out scale	40	39	Out scale
$[Mn(THP)_2(H_2O)_4]$ (E)	Out scale	40	36	45
$[Fe(THP)_2(H_2O)_4]$ (F)	Out scale	43	41	49
Theophylline (S)	--	--	--	--
DMSO	--	--	--	--
$P < 0.01$, highly significant				

Note: Out scale = Outside the limits of the dish.

Conclusions

Each preparation process has advantages and disadvantages such as cost, particle size, aggregation, etc. Our method showed that without aggregation the nano complexes could easily be synthesized. The suggested structure of the nano complexes was octahedral as proved by FTIR, UV-Vis, atomic flame absorption, C/H/N elemental analytics, conductivity, melting point and solubility. According to the TEM calculation, the average size of nano complexes ranged from 9-22 nm. Nano complexes applied to different types of bacteria had a high inhibition zone for each type.

Acknowledgments

This work was supported by Department of Chemistry, College of Science, Mustansiriyah University.

Conflict of Interests

The authors declare that there is no conflict of interest.

References

[1] N.J. Farrer, L. Salassa, P.J. Sadler, Photoactivated chemotherapy (PACT): the potential of excited-state d-block metals in medicine. Dalton Transactions. 2009(48):10690-10701.

[2] A.A. Zaid, M. Mohsin, M. Farooqui, et al, Effect of ionic strength on the stabilities of ciprofloxacin

[3] Metal complexes. Journal of Saudi Chemical Society. 2013, 17(1): 43-45.

[4] C. Garino, L. Salassa. The photochemistry of transition metal complexes using density functional theory. Philosophical Transactions of the Royal Society A: Mathematical, Physical and Engineering Sciences. 2013, 71(1995): 20120134.

[5] C. Daniel. Photochemistry and photophysics of transition metal complexes: Quantum chemistry. Coordination Chemistry Reviews. 2015, 282: 19-32.

[6] M. Litecká, R. Gyepes, Z. Vargová, et al., Toxic metal complexes of macrocyclic cyclen molecule-synthesis, structure and complexing properties. Journal of Coordination Chemistry. 2017, 70(10): 1698-1712.

[7] A.H. Ismail, H.K. Al-Bairmani, Z.S. Abbas, et al., Nano-synthesis, spectroscopic characterisation and antibacterial activity of some metal complexes derived from Theophylline. Egyptian Journal of Chemistry. 2020, 63(7): 1-5.

[8] A.M. Rheima, M.A. Mohammed, S.H. Jaber, et al. Adsorption of selenium (Se^{4+}) ions pollution by pure rutile titanium dioxide nanosheets electrochemically synthesized. Desalination and Water Treatment. 2020, 194: 187-193.

[9] A.M. Rheima, M.A. Mohammed, S.H. Jaber, et al., Synthesis of silver nanoparticles using the UV-irradiation technique in an antibacterial application. Journal of Southwest Jiaotong University, 2019, 54(5): 1-11.

[10] A.M. Mohammed, A.M. Rheima, S.H. Jaber, et al., The removal of zinc ions from their aqueous solutions by Cr_2O_3 nanoparticles synthesized via the UV-irradiation method. Egyptian Journal of Chemistry, 2020, 1: 425-431.

[11] A.M. Rheima, M.A. Mohammed, S.H. Jaber, et al., Inhibition effect of silver-calcium nanocomposite on alanine transaminase enzyme activity in human serum of Iraqi patients with chronic liver disease. Drug Invention Today, 2019, 12(11): 2818-2821.

[12] A.A. Ali, R.M. Al-Hassani, D.H. Hussain, et al., Synthesis, spectroscopic, characterization, pharmacological evaluation, and cytotoxicity assays of novel nano and micro scale of copper (II) complexes against human breast cancer cells. Drug Invention Today, 2020, 14(1): 31-39.

[13] D.H. Hussain, A.M, Rheima, and S.H. Jaber., Cadmium ions pollution treatments in aqueous solution using electrochemically synthesized gamma aluminum oxide nanoparticles with DFT study. Egyptian Journal of Chemistry, 2020, 63(2): 417-424.

[14] A.A. Ali, R.M. Al-Hassani, D.H. Hussain, et al., Fabrication of solar cells using novel micro-and nano-complexes of triazole Schiff base derivatives. Journal of Southwest Jiaotong University, 2019, 54(6): 1-19.

[15] A.M. Rheima, D.H. Hussain, and M.M. Almijbilee, Graphene-silver nanocomposite: synthesis, and adsorption study of Cibacron blue dye from their aqueous solution. Journal of Southwest Jiaotong University. 2019, 54(6): 1-8.

[16] D.H. Hussain, H.I. Abdulah, and A.M. Rheima. Synthesis and characterization of γ-Fe_2O_3 nanoparticles photo anode by novel method for dye sensitized solar cell. International Journal of Scientific and Research Publications. 2016, 6(10): 26-31.

[17] S.H. Jabber, D.H. Hussain, A.M. Rheima, et al., Comparing study of CuO synthesized by biological and electrochemical methods for biological activity. Al-Mustansiriyah Journal of Science, 2019, 30: 94-98.

[18] A.M. Rheima, D.H. Hussain, and H.I. Abdulah, Silver nanoparticles: Synthesis, characterization and their used a counter electrodes in novel Dye sensitizer solar cell. IOSR Journal of Applied Chemistry, 2016, 9: 6-9.

[19] H.I. Abdulah, D.H. Hussain, and A.M. Rheima. Synthesis of α-Fe_2O_3, γ-Fe_2O_3 and Fe_3O_4 nanoparticles by electrochemical method. Journal of Chemical, Biological and Physical Sciences, 6(4): 1288-1296

[20] A.H. Ismail, H.K. Al-Bairmani, Z.S. Abbas, et al., Nanoscale synthesis of metal (II) theophylline complexes and assessment of their biological activity. Nano Biomed. Eng., 2020, 12(2): 139-147.

[21] T.J. Kistenmacher, D.J. Szalda, and L.G. Marzilli, Intercalative stacking interactions and interligand hydrogen bonding in metal purine complexes. Crystal and molecular structure of (Nsalicylidene-N'-methylethylenediamine)(theophyllinato)copper (II) monohydrate. Inorg. Chem., 1975, 14: 1686-1691.

[22] E. H. Hamdani, E. Amane, and C. Duhayon. Crystal structure of tetraaquabis (1,3-dimethyl-2,6-dioxo-7H-purin-7-ido-κN7) cobalt (II). Acta Crystallographica Section E: Crystallographic Communications. 2017, 73(9): 1302-1304.

[23] J. Lorberth, W. Massa, E. Essawi, et al., Trimethylplatinum-theophylline hexamer: A novel Pt6 heterocycle containing both Pt- N and Pt- O bonds. Angewandte Chemie International Edition in English, 1988, 27(9): 1160-1161.

[24] M. Gacki, K. Kafarska, A. Pietrzak, et al., Synthesis, characterisation, crystal structure and biological activity of metal (II) complexes with theophylline. Journal of Saudi Chemical Society, 2019, 23(3): 346-354.

[25] M.S. Refat, H.K. Ibrahim, S.Z. Sowellim, et al., Spectroscopic and thermal studies of Mn(II), Fe(III), Cr(III) and Zn(II) complexes derived from the ligand resulted by the reaction between 4-Acetyl Pyridine and Thiosemicarbazide. Journal of Inorganic and Organometallic Polymers and Materials, 2009, 19(4): 521.

Copyright© Ahmad Hussein Ismail, Hassanain Kamil Al-Bairmani, Zainab Sabri Abbas, and Ahmed Mahdi Rheima. This is an open-access article distributed under the terms of the Creative Commons Attribution License, which permits unrestricted use, distribution, and reproduction in any medium, provided the original author and source are credited.